



DOI: 10.18720/MCE.100.6

The formation mechanism of the porous structure of glass ceramics from siliceous rock

V.T. Erofeev^a, A.I. Rodin^{*a}, V.S. Bochkin^b, A.A. Ermakov^a

^a Ogarev Mordovia State University, Saransk, Respublika Mordoviya, Russia,

^b LLC "Kombinat teploizolyacionnyh izdelij", Saransk, Respublika Mordoviya, Russia,
E-mail: al_rodin@mail.ru

Keywords: glass ceramics, silicates, pore structure, differential thermal analysis, compressive strength, microstructure, mechanical activation

Abstract. Porous glass ceramic materials are widely used in industrial and civil engineering due to a number of redeeming features, such as high strength, low thermal conductivity, incombustibility, environmental friendliness, etc. A large number of researches are devoted to developing the compositions of foam glass ceramic materials based on siliceous rocks (diatomite, tripoli, opoka). Present article is devoted to studying the formation mechanism of the porous structure of glass ceramic materials as a result of heating a mechanically activated mixture (a mixture of siliceous rock and soda ash or thermonatrite). The experimental results were obtained using methods of gas permeability, scanning electron microscopy (SEM), infrared spectroscopy (IR), X-ray diffraction analysis (XRD), differential thermal analysis (DTA) and differential thermal gravimetric (DTG) analysis, physical-mechanical and thermophysical tests. It was determined that the minerals of the crystalline structure in the composition partially transfer to the amorphous phase with an increase in the charge activation time, and the amount of heulandite and sodium hydrosilicates increases. This contributes to an intensive increase in the amount of flux in the composition within the temperature range 700–800 °C. The water vapor generated during the condensation of free OH groups on the surface of silicate is formed in this temperature range. This is the formation source of the material's porous structure. The developed porous glass ceramic materials have increased compressive strength (up to 5 MPa) at a relatively low average density (268.5 kg/m³). This is several times greater than the strength of foam glass from waste glass and from fly or coal ash. The minimum thermal conductivity of glass ceramics (0.0633 W/m·°C) was determined at a sample density of 220.7 kg/m³. The maximum operational temperature of the material was 850 °C, which allows using it as a thermal insulation of industrial equipment, such as melting furnaces, boiler equipment, etc.

1. Introduction

There are a large number of studies in the world scientific literature, which are devoted to developing compositions and studying properties of porous glass ceramics. According to studies, such materials have high strength, low thermal conductivity, are incombustible and ecologically safe [1–2]. They have proven themselves in industrial and civil engineering [3]. A large number of studies in recent years are devoted to the development of foam glass ceramic materials made of waste glass and various ashes [4–6]. Some researches are related to studying the foaming of a charge by introducing MnO₂ into the composition [7, 8]. The structural formation peculiarities and the mechanical properties of glass ceramics from slags of various metallurgical industries, as well as from copper slags [11], lead-zinc mine tail ends, red mud [12] and many others were studied [9, 10]. A large number of researches are devoted to developing the compositions of foam glass ceramic materials from siliceous rocks (diatomite, tripoli, opoka) [13–22]. The technology for producing such materials is mainly mixing siliceous and zeolite-containing rocks with aqueous solutions of NaOH, followed by granulation and burning.

Erofeev, V.T., Rodin, A.I., Bochkin, V.S., Ermakov, A.A. The formation mechanism of the porous structure of glass ceramics from siliceous rock. Magazine of Civil Engineering. 2020. 100(8). Article No. 10006. DOI: 10.18720/MCE.100.6



This work is licensed under a CC BY-NC 4.0

According to the studies [16, 17], sodium hydrosilicates are formed when siliceous rocks are mixed with aqueous solutions of NaOH. When heated, these compounds are dehydrated, and the water vapor released during dehydration forms the porous structure of the material. The foaming intensity of zeolite-containing rocks activated with aqueous NaOH solutions depends on the rock fineness and on presence of zeolites in the composition of minerals that contain Ca in the structure [16]. According to [16, 17], zeolite minerals dehydrate with blockage in the micropores of surface hydroxyl groups (Si–O–H) when heating the charge to 700 °C. Increasing the heating temperature leads to the condensation of such hydroxyl groups with release of water vapor, which forms the porous structure of material. According to the research results [17, 22], the porosity of glass ceramic materials also occurs due to the release of CO₂ at temperatures above 700 °C. However, scientific literature contains ambiguous opinions regarding the nature of CO₂ formed when heating siliceous rocks above 700 °C, activated by alkaline solutions. One theory [17] is that carbon dioxide is released due to decarbonization of the formed Na₂CO₃. Other sources have shown [22] that pore formation occurs due to the release of carbon dioxide from CaCO₃. There is also a theory that CO₂ is released from the structure of silicates. It was determined that amorphization and carbonization of minerals occur during long-term grinding of silicates and aluminosilicates of alkaline earth metals [23, 24]. Carbon dioxide is in the structure of the material in a form similar to dissolved CO₂ in silicate glasses, obtained at high temperature and pressure.

Analyzing the above mentioned, it can be concluded that porous glass ceramic from siliceous rock is obtained mainly by mixing the rock with an aqueous solution of NaOH followed by burning [14–17, 22]. However, the equipment deteriorates rapidly with this production technology, as a result of exposure to alkalis. Moreover, burning the charge is accompanied with the release of harmful substances (NaOH) into the atmosphere [18]. Therefore, the production of these materials is limited to small batches only. It is possible to solve this issue by replacing the alkaline solution with alkali metal salts in dry form, such as soda ash (Na₂CO₃) or thermonatrite (Na₂CO₃·H₂O). It is advisable to mix the components by co-grinding (mechanical activation). The results of studies on developing the compositions of porous glass ceramic materials from mechanically activated siliceous rocks and soda ash were presented by authors [25]. The pore formation mechanism of such materials has not yet been studied.

The goal of research is to study the formation mechanism of the porous structure of glass ceramic materials as a result of heating a mechanically activated mixture (a mixture of siliceous rock and soda ash or thermonatrite).

Objectives:

- to determine the impact of mechanical activation time on the change in the specific surface, phase composition, shape and size of the charge particles;
- to determine the formation mechanism of the porous structure of glass ceramics by the methods of infrared (IR) spectroscopy, thermal analysis (TA) and X-ray diffraction analysis (XRD);
- to determine the impact of the charge's mechanical activation time on the physical, mechanical and thermophysical properties of porous glass ceramic samples.

2. Methods

2.1. Materials

The charge components in order to obtain samples of foam glass materials are as follows:

- siliceous rock (humidity ≤ 1 %) with the following chemical composition: SiO₂ – 67.862 %, CaO – 7.742 %, Al₂O₃ – 7.609 %, Fe₂O₃ – 1.987 %, K₂O – 1.561 %, MgO – 1.073 %, TiO₂ – 0.340 %, Na₂O – 0.167 %, P₂O₅ – 0.151 %, SO₃ – 0.059 %, SrO – 0.055 %, BaO – 0.022 %, ZrO₂ – 0.013 %, V₂O₅ – 0.012 %, MnO – 0.009 %, Cr₂O₃ – 0.008 %, CuO – 0.004 %, ZnO – 0.004 %, NiO – 0.004%, Co₃O₄ – 0.003%, other impurities – 11.315 %. The mineralogical composition of the rock is as follows: cristobalite (SiO₂) – 21.1 %, heylandite ((Ca,Sr,K₂,Na₂)[Al₂Si₆O₁₆]·5H₂O) – 19.2 %, muscovite (KAl₂[AlSi₃O₁₀](OH)₂) – 14.4 %, calcite (CaCO₃) – 12.8 %, quartz (SiO₂) – 10.8 %, tridymite (SiO₂) – 1.7 %, amorphous phase – 20.0%.
- flux agents: technical soda ash (mineral – natrite, chemical formula – Na₂CO₃); thermonatrite (chemical formula – Na₂CO₃·H₂O). Mass fraction of the main substance in both components is not less than 99 %.

2.2. Compositions and technology for the production of samples

The mixture for producing the samples of foam glass ceramic materials was obtained by co-grinding siliceous rock and flux agent (Na₂CO₃ or Na₂CO₃·H₂O). The amount of flux agent was adopted as 18.5 %

of the charge mass in terms of the main substance, which is Na_2CO_3 . The grinding was carried out in a planetary ball mill Retsch PM 400 at a rotational speed of milling pots equal to 250 rpm.

Samples of foam glass ceramic materials were obtained by burning the charge in metal forms in a muffle furnace. The forms were pretreated with kaolin paste. The following charge burning mode was adopted: heating to a temperature of 670 °C at the 4.5 °C/min rate, holding at a temperature of 670 °C for 1 hour, heating to a temperature of 850 °C at a speed of 4.5 °C/min, holding at a temperature of 850 °C for 30 minutes. After cooling the mold with obtained material together with the furnace down to 40 °C, the mold was disassembled, and samples were removed for further testing.

The compositions tested in the study are presented in Table 1.

Table 1. Compositions tested in the study.

Composition number	Charge composition, %			Mechanical activation time, min
	Siliceous rock	Na_2CO_3	$\text{Na}_2\text{CO}_3 \cdot \text{H}_2\text{O}$	
C1				10
C2				30
C3	81.5	18.5	-	60
C4				90
C5				120
C6				10
C7				30
C8	79	-	21	60
C9				90
C10				120

2.3. Analytical techniques

The experimental data was obtained by using following methodologies:

- Specific surface of the charge was determined by the gas permeability method using the PSH-2 device. The arithmetic mean value of the test results for three samples of each composition was adopted as the final result.

- Scanning electron microscopy (SEM) of powdered charge samples was carried out using a Quanta 200 i 3D device (USA) in a low vacuum mode (10^{-3} Pa) with an accelerating voltage of 20 kV and a working distance of 15 mm.

- XRD of the unburnt and burnt charge samples was carried out using an ARL X'tra diffractometer (Switzerland). Samples of the burnt charge were crushed in a mortar with an agate pestle with acetone before passing through a sieve with an aperture of 90 μm . The diffraction patterns were recorded in $\text{CuK}\alpha_{1+2}$ radiation in the angle range $2\theta = 4-80^\circ$ with a rate of 1.2 $^\circ/\text{min}$, in increments of 0.02 $^\circ$, integration time 1 sec. The qualitative phase composition of samples was determined according to the Hanawalt method using the ICDD PDF-2 database. The quantitative phase content was determined according to the Rietveld method using Siroquant 3 Sietronics Pty Ltd software.

- TA of charge samples was carried out using a TGA/DSC1 device (Switzerland). 15 ± 0.1 mg of charge was poured into an alundum pot with a volume of 150 μl . After that, the sample was compacted by tapping the pot on the table. The pot was mounted on a holder and placed in an oven. The sample was heated from 30 to 800 °C at a rate of 10 °C/min.

- IR spectra were obtained in KBr pellets on the InfraLUM FT-02 Fourier spectrometer. In order to prepare the pellets, 3 mg of the sample and 200 mg of single-crystal KBr were used, the mixture was thoroughly ground in an agate mortar, and then the pellets were pressed. Spectral absorption curves of the sample were recorded in the range from 400 to 4000 cm^{-1} .

- Density, compressive strength, water absorption and thermal conductivity of foam glass ceramic materials were determined using dry cubic samples with a face size of 90 ± 5 mm. Water absorption was determined using the ratio of water mass absorbed by dry sample to the sample volume when completely immersed in water for 24 hours. The thermal conductivity of samples was determined by probe method using the MIT-1 device (probe diameter 6 mm). The final result was adopted as the arithmetic mean value of the test results for five samples of each composition.

- Maximum operating temperature of the glass ceramic materials was determined by the residual change in the size of the samples (90x40x40 mm) after holding for 2 hours at a given temperature. The

test was aborted if the sample size changed by more than 1 %. The arithmetic mean value of the test results for three samples of each composition was taken as the final result.

3. Results and Discussion

3.1. Charge properties

It is known that the morphological and dimensional characteristics of charge significantly impact the quality of finished goods regarding production of porous glass ceramic materials. The macrostructure of the material becomes homogeneous with decreasing charge particle size, density decreases, strength increases, etc. [26–28]. Within the framework of research, the correlation between change in the specific surface area of charge powder samples (siliceous rock + flux agent) and the time of mechanical activation were determined. Results are presented in Figure 1.

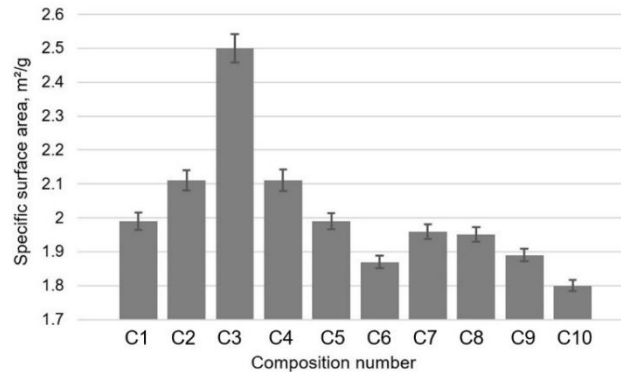


Figure 1. Specific surface of the charge samples.

According to the obtained data (Figure 1), specific surface of charge samples, which contains soda ash as flux agent, increases almost linearly from 1.99 to 2.50 m²/g. The mechanical activation time increases from 10 to 60 minutes at the same time. By increasing the activation time to 120 min, specific surface of the charge decreases in an inverse linear relationship to 1.99 m²/g.

There are no sharp changes regarding the specific surface values during mechanical activation of the mixture (compositions C6–C10, thermonatrite as a flux agent). The highest indicator value for compositions C7 and C8 (30 and 60 min, respectively) is 1.95 m²/g on average. That is more than 20 % lower than the same indicator for the composition with Na₂CO₃ (C3 composition). A further increase in the mechanical activation time up to 120 min leads to a decrease in the specific surface area of charge to 1.8 m²/g. Most likely this is due to the aggregation of charge particles, and the water molecules contained in the thermonatrite composition contribute to this. Microstructural changes in the charge samples after mechanical activation are presented in Figure 2.

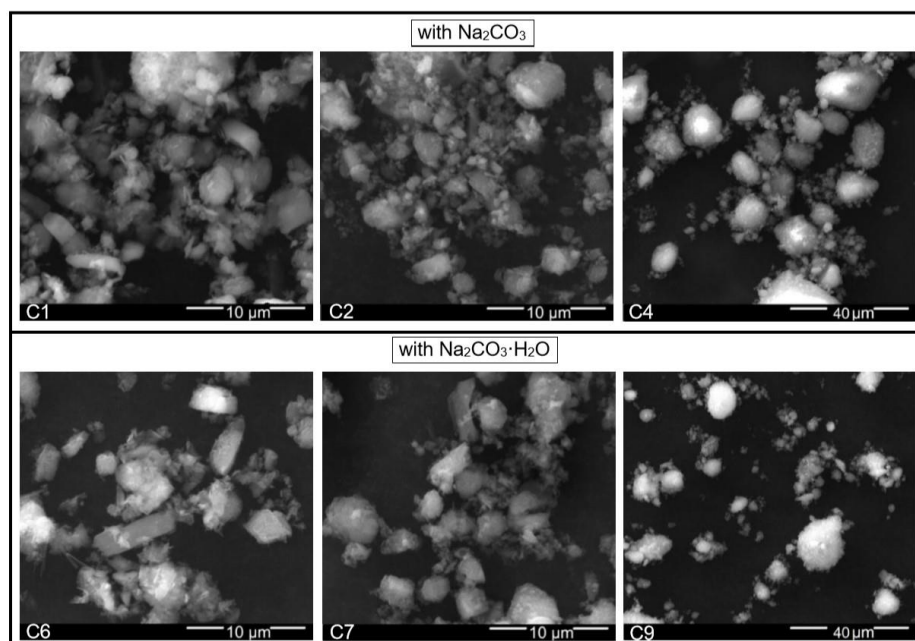


Figure 2. SEM-micrographs of charge samples.

SEM microstructure images of the charge powder samples (Figure 2) clearly demonstrate the effect of mechanical activation duration on the shape and size changes of particles of the starting materials, as well as of newly formed aggregates. After 10 min of mechanical activation (C1, C6), all charge particles have size of no more than 10 μm , regardless of flux agent type in the composition. The shape of most particles is shard with almost no aggregation.

After 30 minutes of mechanical activation of the charge containing soda ash (C2) as flux agent, the particle size decreased compared to sample C1 (10 minutes of mechanical activation). The composition is dominated by shard-shaped particles of size less than 3 μm , as well as by individual spherical aggregates of size less than 5 μm . The particle shape of sample C7 (flux agent is termonatrite) is represented by fragmentary and loose polydisperse aggregates no larger than 5 μm in size. The particle size slightly decreased comparing with C6 sample (10 min of mechanical activation).

With increasing the mechanical activation duration of the charge samples up to 90 min, a significant difference was noted regarding the sizes of the formed aggregates. For sample C4 (flux agent is soda ash), the most of spherical aggregates are 10–15 μm in size. For sample C9 (flux agent is termonatrite), all particles in the form of spherical polydisperse aggregates are not more than 15 μm .

As a result of the study, it was determined that mechanical activation significantly affects the shape of the charge particles in the mixture. Spherical aggregates are formed, the size of which increases with the activation time. The dispersion of aggregates depends on the flux agent type in the composition. The SEM results for the charge are correlated with data on its specific surface area obtained by gas permeability method.

According to the scientific literature, structural defects accumulate in solid particles during intensive grinding, phase transformations occur, as well as amorphization of crystalline minerals [23, 24, 26–28]. The impact of the mechanical activation time on structural changes in the charge for foam glass ceramic has been studied using IR spectroscopy and XRD methods.

The IR spectra of the charge samples after mechanical activation for 10 and 90 minutes are presented in Figure 3.

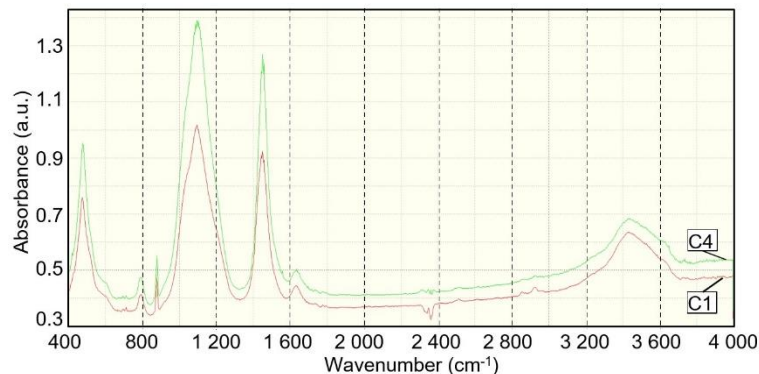


Figure 3. IR spectra of charge samples.

The presence of silicates with different structural types in the tested samples can be detected by using the following absorption bands in the IR spectra (see Figure 3). Intense absorption bands with maxima $\approx 1100 \text{ cm}^{-1}$ and $\approx 470 \text{ cm}^{-1}$ belong to the stretching and deformation vibrations of the Si–O–Si bonds, respectively. The absorption spectrum with a peak $\approx 1050 \text{ cm}^{-1}$, corresponding to stretching vibrations of the Si–O–Si(Al) bonds is clearly visible in the IR spectrum of sample C1. The $\approx 1200 \text{ cm}^{-1}$ band, which indicates the presence of a whole set of structures with Si–O–Si angles $\approx 180^\circ$, is visible as well. According to [29], the absorption band of $\approx 1200 \text{ cm}^{-1}$ appears during quartz fracture, and a decrease in its intensity in the sample's IR spectrum after 90 min mechanical activation (sample C4) is probably a result of $\beta\text{-SiO}_2$ mineral amorphization.

The presence of aluminosilicates in the tested samples can be indicated by changes in the absorption bands intensity $\approx 795 \text{ cm}^{-1}$ (stretching vibrations of the Si–O–Si(Al) bonds), as well as for the bands $\approx 520 \text{ cm}^{-1}$ and $\approx 620 \text{ cm}^{-1}$ (deformation vibrations of the bonds Si–O–Al). Significant changes in the intensity of the absorption bands or frequency of oscillations were not detected.

No significant changes were detected in the vibrational frequency and intensity of the absorption bands $\approx 1460 \text{ cm}^{-1}$, as well as $\approx 880 \text{ cm}^{-1}$ and $\approx 710 \text{ cm}^{-1}$ related to stretching and deformation vibrations in carbonates, respectively.

According to the data in Figure 3, the main changes in the IR spectra of the charge samples after mechanical activation relate to the absorption bands of hydroxyl groups and water molecules.

The absorption band $\approx 1680 \text{ cm}^{-1}$ corresponds to deformation vibrations of water molecules. A wide peak in the range of $3200\text{--}3700 \text{ cm}^{-1}$ demonstrates the superposition of stretching vibration bands of hydroxyl groups and adsorbed H_2O molecules. The intensity of the absorption bands of water molecules in the C4 sample spectrum is slightly lower. This is possibly due to the hydration processes occurred in the charge sample after mechanical activation for 90 min. Such conclusion can be confirmed by an increase in the intensity of absorption band in the range of $980\text{--}880 \text{ cm}^{-1}$ (deformation vibrations of Si-O-H), as well as $\approx 3740 \text{ cm}^{-1}$ (stretching vibrations of surface OH groups in Si-O-H). An increase in the intensity of band $\approx 3650 \text{ cm}^{-1}$ indicates an increase in the number of associated OH groups in Si-O-H .

When analyzing the IR spectra, the absorption bands of carbon dioxide in the range of $2300\text{--}2400 \text{ cm}^{-1}$ were not taken into account, these bands are inevitable consequence of the experimental error (air CO_2).

The XRD of the charge samples after mechanical activation is shown in Figure 4.

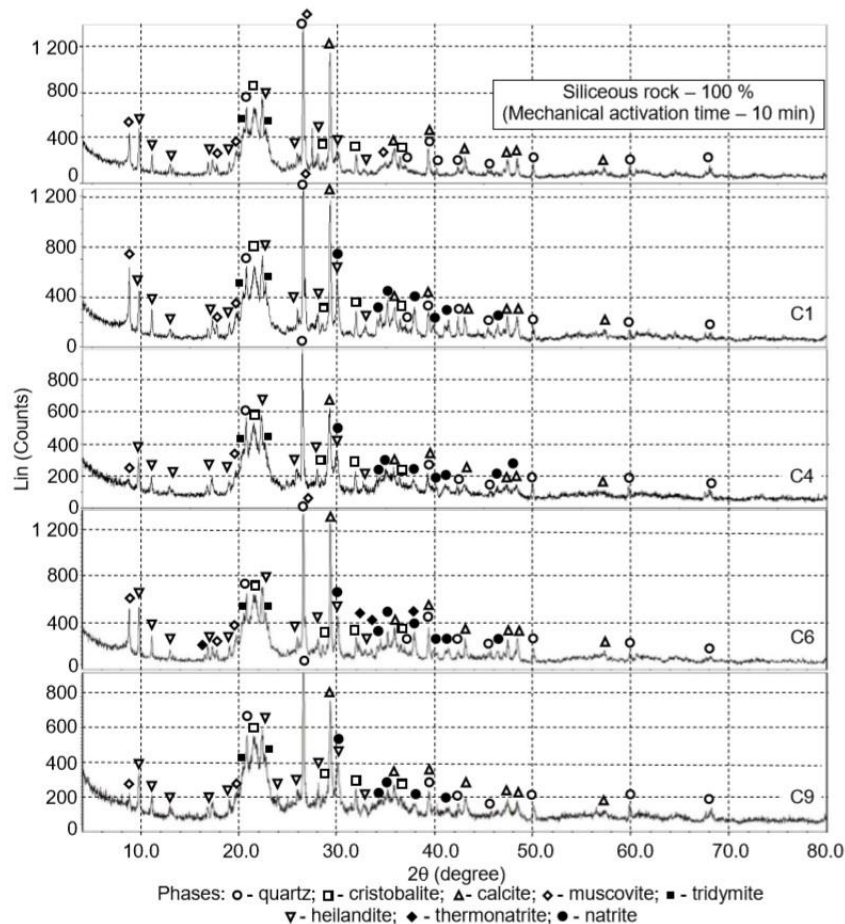


Figure 4. XRD of the charge samples.

According to the data presented in Figure 4, the main changes in the charge's phase composition after mechanical activation are as follows. With an increase in mechanical activation time of the charge, the intensity decreases and the peaks corresponding to calcite, muscovite, quartz, and cristobalite widens. Similar effects appear during the amorphization of crystalline minerals. With an increase in the mechanical activation time, the amount of Na_2CO_3 and $\text{Na}_2\text{CO}_3 \cdot \text{H}_2\text{O}$ decreases significantly. The content of the latter in the charge composition after 90 min of activation was not detected (C9). In parallel, an increase in the intensity of lines corresponding to heilandite is observed. In the X-ray diffraction patterns of samples C4 and C9 (90 min mechanical activation), a wide halo additionally appears in the range $33\text{--}39^\circ$ (2θ). This effect can be attributed to sodium hydrosilicates formed in the charge [16, 17, 23]. An increase of compounds containing OH groups in the charge composition is also evidenced by the data of IR spectroscopy (Figure 3).

3.2. Formation mechanism of the porous structure

The phase transformations occurring in the charge samples after mechanical activation by heating were studied using DTA and DTG methods. Results of the study are presented in Figure 5. The total weight loss of the samples after burning at a temperature of 800°C is shown in Table 2.

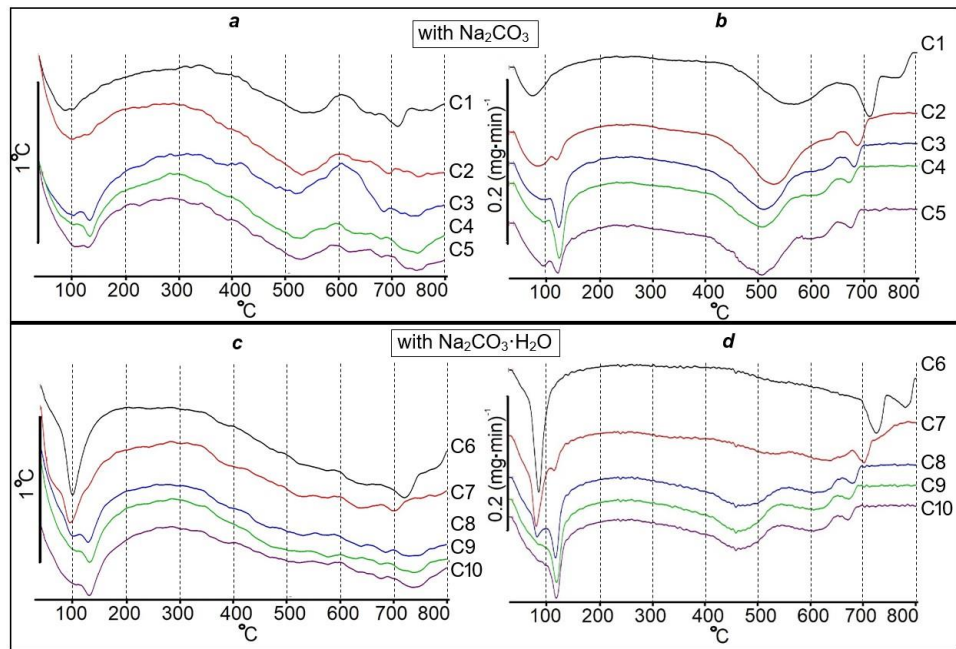


Figure 5. DTA (a, c) and DTG (b, d) curves of charge samples.

Table 2. Weight loss by the charge samples after burning at a temperature of 800 °C.

Composition number	C1	C2	C3	C4	C5	C6	C7	C8	C9	C10
Sample weight loss, %	16.57	17.49	18.04	17.94	17.49	18.88	19.09	19.17	19.00	18.29

According to data presented in Figure 5 and in Table 2, there are following phase transformations occurring in the charge during heating. The first wide peak in the temperature range from 25 to 120 °C (endoeffect) corresponds to the evaporation of unbound water, irrespective of the flux agent type in the composition. An additional peak of strong intensity appears at a maximum of ≈ 95 °C on the DTA (endoeffect) and DTG curves (weight loss) (charge with $\text{Na}_2\text{CO}_3 \cdot \text{H}_2\text{O}$), corresponding to dehydration of thermonatrite. It should be noted that a peak with a maximum of ≈ 95 °C gradually disappears with an increase in the mechanical activation time from 10 to 90 minutes. Moreover, new endothermic effect (Figure 5, a, c) appears at a temperature of ≈ 120 °C, accompanied by weight loss. This effect may be associated with the loss of water from the resulting sodium hydrosilicates. An increase in the amount of these compounds with increasing the charge activation time most likely led to the formation of aggregation of charge particles (Figure 2). The almost total absence of thermonatrite after 90 minutes of mechanical activation is confirmed by XRD data (Figure 4).

The strong endothermic effect and significant weight loss of the samples in the temperature range from 400 to 550 °C is a consequence of the formation of sodium silicates. A similar result was obtained in studies [17, 25]. The effect is accompanied with the release of carbon dioxide and water vapor from individual phases of the charge (CaCO_3 , Na_2CO_3 , etc.). Peak of the effect shifts towards lower temperatures by more than 50 °C with an increase in the time of mechanical activation of the charge from 10 to 90 minutes, respectively. This is due to an increase in the amorphous phase in the composition (Figure 4).

The endoeffect and weight loss in the temperature range from 550 to 650 °C is associated with the release of water vapor during the condensation of OH groups. Similar effect was observed when burning zeolite-containing rocks activated by alkaline solutions [16]. According to the data of various researchers [16, 17, 23], blockage in the micropores of surface hydroxyl groups (Si–O–H) occurs in this temperature range. Based on data presented in Figure 5, peak intensity and mass loss are greater for composition with thermonatrite. This is logical, since thermonatrite consists of H_2O molecules by almost 14.5 %, the molecules are necessary for the formation of OH groups.

According to Figure 5, the endothermic effect with a peak of ≈ 720 °C (decarbonization of unreacted CaCO_3) for compositions C1 and C6 (10 minutes of mechanical activation) shifts by more than 50 °C to lower temperatures after mechanical activation for ≥ 60 minutes.

Mechanical activation duration of the charge also affects the increase in the amount of flux agent in the composition. Confirmation for this is the increase in the endothermic effect in the temperature range 700–800 °C with an increase in activation time to 120 minutes. According to the study [22], an eutectic flux

appears in the $\text{Na}_2\text{O}-\text{CaO}-\text{SiO}_2$ system in this temperature range. The effect is characterized by the weight loss absence in the sample, as evidenced by a straight line on the DTG curves (samples C3–C5, C8–C10). The mixture foams in this temperature range, but only after mechanical activation for 1 hour or more.

The surface macrostructure of porous glass ceramic samples, which are based on charge after mechanical activation of different durations, is presented in Figure 6.

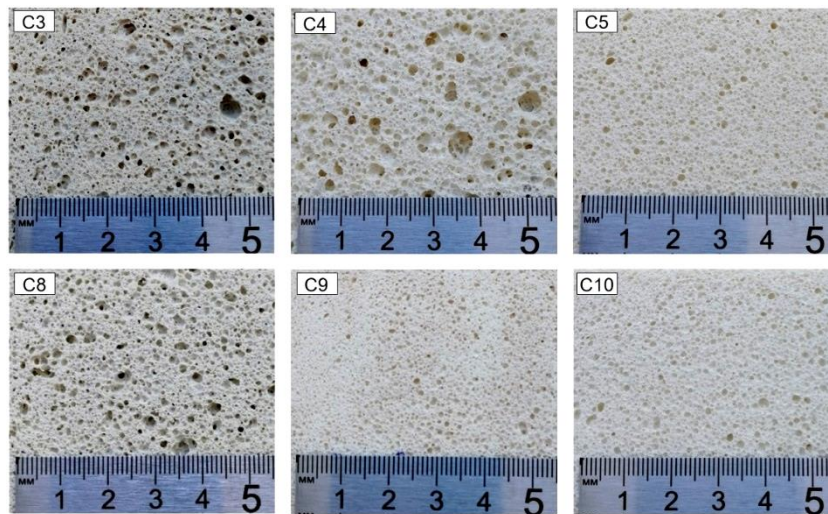


Figure 6. Surface macrostructure of foam glass ceramic samples.

According to the data in Figure 6, it is possible to obtain the optimal porous structure in the samples of foam glass ceramic materials (pore diameter no more than 2 mm) from the presented siliceous rock. However, the rock has to be mechanically activated with $\text{Na}_2\text{CO}_3 \cdot \text{H}_2\text{O}$ (21 % of the charge mass) for at least 90 minutes (samples C9, C10), together with at least 120 minutes of Na_2CO_3 (18.5% of the charge mass) (sample C5).

According to the data presented in Table 3, total weight loss of the sample after burning at a temperature of 800 °C decreases by more than 1 % for a charge with thermonatrite. This occurs in case the mechanical activation duration of the charge is increased for more than 1 hour. Theoretically, this phenomenon is unlikely, since the charge activation was carried out in a closed system. Perhaps, this effect is caused by the part of volatile substances (CO_2 and/or H_2O), which are still in the charge composition and form the porous structure in the glass ceramic samples. As noted above, the process of pore formation in the production of glass ceramic materials can be associated with the release of water vapor during the condensation of free OH groups on the silicate surface [16, 17, 22]. This is a result of decarbonization of CaCO_3 [22], Na_2CO_3 [16] or carbon dioxide from the structure of silicates [23, 24]. In order to confirm any of the mentioned assumptions, the charge samples were tested by XRD and IR spectroscopy after burning at a temperature of 670 °C. The maximum burning temperature (670 °C) was selected based on the thermal analysis data of the charge samples presented above. The burnt samples were milled in an inert gas (argon) in order to exclude the possibility of CO_2 re-entering the silicate structure. The results of the XRD are presented in Figure 7.

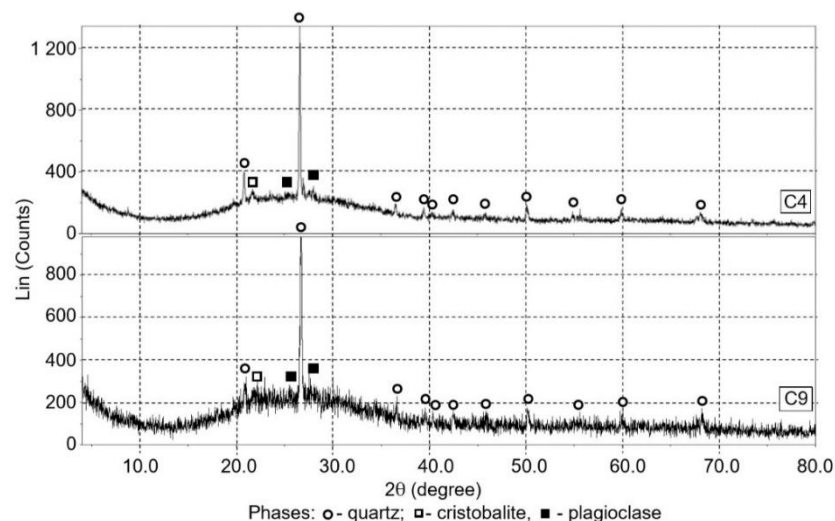


Figure 7. XRD of the charge samples after burning at a temperature of 670 °C.

As a result of the X-ray diffraction analysis of the charge samples after burning at a temperature of 670 °C (Figure 7), the following was determined. Regardless of the flux agent type in the initial charge composition (Na_2CO_3 or $\text{Na}_2\text{CO}_3 \cdot \text{H}_2\text{O}$), the crystalline phase of the burnt samples is mainly represented by quartz. There are individual peaks on radiographs, corresponding to cristobalite and plagioclases. Figure 7 clearly shows an intense amorphous halo in the angle range from 15 to 37° (2θ). The absence of peaks on the X-ray diffraction pattern is determined. These peaks characterize the presence of Na_2CO_3 , CaCO_3 in the composition of samples, as well as other minerals of a crystalline structure that could be involved in the pore formation process.

The final conclusions regarding the possible pore formation cause in the production of porous glass ceramic materials (free OH groups on the surface of silicate [16, 17, 22] or carbon dioxide in the structure of silicates [23, 24]) were made according to the results of IR spectroscopy (Figure 8).

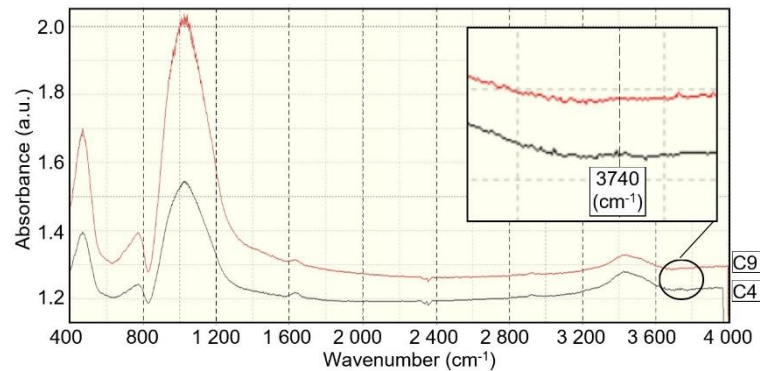


Figure 8. IR spectra of burnt charge samples at a temperature of 670 °C.

According to the IR spectra analysis (Figure 8) of the charge samples after burning at 670 °C, the pore formation of glass ceramic materials (based on the siliceous rock used) occurs due to release of water vapor. The vapor is generated by the condensation of free OH groups on the silicate surface. This is confirmed by the absorption band of a very low intensity $\approx 3740 \text{ cm}^{-1}$. A similar character of pore formation in glass ceramic materials is described in various studies [16, 17, 22].

The assumption regarding the possible pore formation process in glass ceramic materials due to carbon dioxide emission from the structure of silicates [23, 24] has not been confirmed. According to the IR spectra of the charge samples after firing at 670 °C, there are no absorption bands in the range of 1550–1400 cm^{-1} . They are common for stretching vibrations of carbonate groups (samples C4, C9).

When analyzing the IR spectra, absorption bands of carbon dioxide (2300–2400 cm^{-1}) were not taken into account, as well as water molecules ($\approx 1680 \text{ cm}^{-1}$, 3200–3700 cm^{-1}), which are an inevitable consequence of the experimental error (CO_2 from air, H_2O in KBr).

3.3. Properties of samples of foamed glass ceramic materials

The results of studying physical, mechanical and thermophysical properties of porous glass ceramic samples are represented in Table 3.

Table 3. Properties of samples of foam glass ceramic materials.

Composition number	Properties*				
	Average density, kg/m^3	Compressive strength, MPa	Water adsorption, %	Thermal conductivity, $\text{W/m}\cdot^\circ\text{C}$	Resizing of samples after holding at temperature 850°C, %
C4	251.5 (6.5)	4.5 (0.11)	35.35 (1.92)	0.0667 (0.0013)	-0.35 (0.02)
C5	243.3 (5.7)	4.2 (0.10)	18.48 (1.17)	0.0659 (0.0014)	-0.31 (0.02)
C9	268.5 (5.9)	5.0 (0.11)	23.03 (1.25)	0.0705 (0.0011)	-0.38 (0.02)
C10	220.7 (6.1)	2.9 (0.08)	24.84 (1.08)	0.0633 (0.0017)	-0.34 (0.02)

* - the mean square deviation is given in brackets

According to the obtained data (Table 3), an increase in the duration of charge mechanical activation leads to the decrease in average density of foam glass ceramic samples. The effect is more noticeable when the charge with thermonatrite is activated. Thus, the average density of C10 composition samples (120 min of activation) is almost 20 % less than the same indicator for composition C9 (90 min of activation).

Compressive strength of the obtained foam glass ceramic samples is linearly dependent on their average density. The highest compressive strength was recorded for composition C9 (5 MPa) with an

average density of samples equal to 268.5 kg/m^3 . To compare [4], the strength of foam glass samples obtained from waste glass and fly ash is 5 times less ($\approx 1 \text{ MPa}$) at a practically equal average density (267.2 kg/m^3). According to the research [6], similar compressive strengths (5 MPa) of foam glass ceramic samples based on waste glass and coal ash were achieved at a material density of $\approx 460 \text{ kg/m}^3$ (70 % higher than the density of the samples we obtained). C10 composition has the lowest value of compressive strength (2.9 MPa) (see Table 4). It should be noted that samples of this composition have the lowest density (220.7 kg/m^3) and, as a result, thermal conductivity ($0.0633 \text{ W/m}\cdot\text{°C}$).

The analysis of the data presented in Table 4 indicates that the water adsorption of the developed materials also depends on the mechanical activation duration of the charge. With an increase in activation duration, water absorption decreases. This is probably due to an increase in the amount of flux agent in the composition (Figure 5), which helps to reduce the number of open pores in the material structure.

Another positive quality of the developed foam glass ceramic materials is their high maximum operating temperature (850 °C). This allows implementing the developed material as a thermal insulation of industrial equipment, such as smelting furnaces, boiler equipment, etc. Considering this indicator, the foam glass is significantly inferior. Its maximum operating temperature rarely exceeds 600 °C [1].

4. Conclusions

1. It was determined that mechanical activation of siliceous rock together with Na_2CO_3 or $\text{Na}_2\text{CO}_3\cdot\text{H}_2\text{O}$ significantly affects the change in the specific surface. It also affects the shape and size of the charge particles and its phase composition:

a. Using the gas permeability and SEM methods, the specific surface area of the charge was determined to increase linearly with an increase in activation time up to 60 min. If the charge mechanical activation is longer, the specific surface area decreases and spherical aggregates are formed in the composition. The size of aggregates increases depending on the activation time.

b. Using the X-ray diffraction and IR spectroscopy methods, it was determined that the increase in charge activation time causes the crystalline structure minerals in composition to partially go into the amorphous phase. The amount of heilandite and sodium hydrosilicates increases in this case.

2. The formation mechanism of the porous structure of glass ceramics when heating the charge (siliceous rock + Na_2CO_3 or $\text{Na}_2\text{CO}_3\cdot\text{H}_2\text{O}$) after mechanical activation is determined:

c. According to the thermal analysis results, silicate formation in the charge begins at a temperature of about 400 °C , the sample weight loss stops almost completely at 670 °C . The intensive increase in the amount of flux agent in the composition was recorded in the temperature range $700\text{--}800 \text{ °C}$.

d. The formation of glass ceramic's porous structure is determined to be caused by the release of water vapor at a temperature of more than 700 °C . Water vapor is formed by the condensation of free OH groups on the silicate surface. A similar pore formation pattern for glass ceramic materials is observed during burning of siliceous (zeolite-containing) rocks activated by alkaline solutions.

e. Obtaining the optimal porous structure in the foam glass ceramic samples (pore diameter no more than 2 mm) from the presented siliceous rock is possible. The rock has to be mechanically activated with $\text{Na}_2\text{CO}_3\cdot\text{H}_2\text{O}$ (21 % of the charge mass) for at least 90 minutes, and also at least for 120 minutes with Na_2CO_3 (18.5% of the charge mass).

3. The developed porous glass ceramic materials have increased compressive strength (up to 5 MPa) at a relatively low average density (268.5 kg/m^3). This is several times greater than the strength of foam glass from waste glass and fly or coal ash. The minimum thermal conductivity at a sample density of 220.7 kg/m^3 was $0.0633 \text{ W/m}\cdot\text{°C}$. The maximum operating temperature of the material is 850 °C , which allows implementing it as a thermal insulation of industrial equipment, such as melting furnaces, boiler equipment, etc.

5. Acknowledgement

The study was conducted using research grant from the Russian Science Foundation (project No. 18-73-00213).

References

1. Fernandes, H.R., Tulyaganov, D.U., Ferreira, J.M.F. Preparation and characterization of foams from sheet glass and fly ash using carbonates as foaming agents. *Ceramics International*. 2009. 35(1). Pp. 229–235. DOI: 10.1016/j.ceramint.2007.10.019.
2. Vatin, N.I., Nemova, D.V., Kazimirova, A.S., Gureev, K.N. Increase of energy efficiency of the building of kindergarten. *Advanced Materials Research*. 2014. No. 953-954. Pp. 1537–1544. DOI: 10.4028/www.scientific.net/AMR.953-954.1537.
3. Gorshkov A.S., Vatin N.I., Rymkevich P.P., Kydrevich O.O. Payback period of investments in energy saving. *Magazine of Civil Engineering*. 2018. 2(78). Pp. 65–75. DOI: 10.18720/MCE.78.5.

4. Bai, J., Yang, X., Xu, S., Jing, W., Yang, J. Preparation of foam glass from waste glass and fly ash. *Materials Letters*. 2014. No. 136. Pp. 52–54. DOI: 10.1016/j.matlet.2014.07.028.
5. Smolii, V.A., Kosarev, A.S., Yatsenko, E.A. Ash-Slag Based Cellular Glass for Energy-Efficient 3-Ply Construction Panels. *Glass and Ceramics (English translation of Steklo i Keramika)*. 2019. 76(3–4). Pp. 105–108. DOI: 10.1007/s10717-019-00143-0.
6. Zhu, M., Ji, R., Li, Z., Wang, H., Liu, L., Zhang, Z. Preparation of glass ceramic foams for thermal insulation applications from coal fly ash and waste glass. *Construction and Building Materials*. 2016. No. 112. Pp. 398–405. DOI: 10.1016/j.conbuildmat.2016.02.183.
7. König, J., Petersen, R.R., Yue, Y. Fabrication of highly insulating foam glass made from CRT panel glass. *Ceramics International*. 2015. 41(8). Pp. 9793–9800. DOI: 10.1016/j.ceramint.2015.04.051.
8. Petersen, R.R., König, J., Yue, Y. The mechanism of foaming and thermal conductivity of glasses foamed with MnO₂. *Journal of Non-Crystalline Solids*. 2015. No. 425. Pp. 74–82. DOI: 10.1016/j.jnoncrysol.2015.05.030.
9. Cao, J., Lu, J., Jiang, L., Wang, Z. Sinterability, microstructure and compressive strength of porous glass-ceramics from metallurgical silicon slag and waste glass. *Ceramics International*. 2016. 42(8). Pp. 10079–10084. DOI: 10.1016/j.ceramint.2016.03.113.
10. Yatsenko, E.A., Gol'tsman, B.M., Kosarev, A.S., Karandashova, N.S., Smolii, V.A., Yatsenko, L.A. Synthesis of Foamed Glass Based on Slag and a Glycerol Pore-Forming Mixture. *Glass Physics and Chemistry*. 2018. 44(2). Pp. 152–155. DOI: 10.1134/S1087659618020177.
11. Yang, Z., Lin, Q., Lu, S., He, Y., Liao, G., Ke, Y. Effect of CaO/SiO₂ ratio on the preparation and crystallization of glass-ceramics from copper slag. *Ceramics International*. 2014. 40(5). Pp. 7297–7305. DOI: 10.1016/j.ceramint.2013.12.071.
12. Liu, T., Li, X., Guan, L., Liu, P., Wu, T., Li, Z., Lu, A. Low-cost and environment-friendly ceramic foams made from lead-zinc mine tailings and red mud: Foaming mechanism, physical, mechanical and chemical properties. *Ceramics International*. 2016. 42(1). Pp. 1733–1739. DOI: 10.1016/j.ceramint.2015.09.131.
13. Erofeev, V., Korotaev, S., Bulgakov, A., Tretiakov, I., Rodin, A. Getting Fired Material with Vitreous Binder Using Frame Technology. *Procedia Engineering*. 2016. No. 164. Pp. 166–171. DOI: 10.1016/j.proeng.2016.11.606.
14. Ivanov, K.S. Granulated foam-glass ceramics for ground protection against freezing. *Magazine of Civil Engineering*. 2018. 3(79). Pp. 95–102. DOI: 10.18720/MCE.79.10.
15. Ivanov, K.S. Optimization of the structure and properties of foam-glass ceramics. *Magazine of Civil Engineering*. 2019. 89(5). Pp. 52–60. DOI: 10.18720/MCE.89.5.
16. Kazantseva, L.K., Rashchenko, S.V. Chemical processes during energy-saving preparation of lightweight ceramics. *Journal of the American Ceramic Society*. 2014. 97(6). Pp. 1743–1749. DOI: 10.1111/jace.12980.
17. Kazantseva, L.K., Rashchenko, S.V. Optimization of porous heat-insulating ceramics manufacturing from zeolitic rocks. *Ceramics International*. 2016. 42(16). Pp. 19250–19256. DOI: 10.1016/j.ceramint.2016.09.091.
18. Mueller, A., Sokolova, S.N., Vereshagin, V.I. Characteristics of lightweight aggregates from primary and recycled raw materials. *Construction and Building Materials*. 2008. 22(4). Pp. 703–712. DOI: 10.1016/j.conbuildmat.2007.06.009.
19. Sokolova, S.N., Vereshagin, V.I. Lightweight granular material from zeolite rocks with different additives. *Construction and Building Materials*. 2010. 24(4). Pp. 625–629. DOI: 10.1016/j.conbuildmat.2009.10.010.
20. Volland, S., Kazmina, O., Vereshchagin, V., Dushkina, M. Recycling of sand sludge as a resource for lightweight aggregates. *Construction and Building Materials*. 2014. No. 52. Pp. 361–365. DOI: 10.1016/j.conbuildmat.2013.10.088.
21. Zhimalov, A.A., Bondareva, L.N., Igitkhanyan, Y.G., Ivashchenko, Y.G. Use of Amorphous Siliceous Rocks – Opokas to Obtain Foam Glass with Low Foaming Temperature. *Glass and Ceramics (English translation of Steklo i Keramika)*. 2017. 74(1–2). Pp. 13–15. DOI: 10.1007/s10717-017-9916-1.
22. Kazantseva, L.K., Lygina, T.Z., Rashchenko, S.V., Tsyplakov, D.S. Preparation of Sound-Insulating Lightweight Ceramics from Aluminosilicate Rocks with High CaCO₃ Content. *Journal of the American Ceramic Society*. 2015. 98(7). Pp. 2047–2051. DOI: 10.1111/jace.13581.
23. Kalinkin, A.M., Kalinkina, E.V., Zalkind, O.A., Makarova, T.I. Mechanochemical interaction of alkali metal metasilicates with carbon dioxide: 1. Absorption of CO₂ and phase formation. *Colloid Journal*. 2008. 70(1). Pp. 33–41. DOI: 10.1007/s10595-008-1006-1.
24. Kalinkin, A.M., Kalinkina, E.V., Zalkind, O.A., Makarova, T.I. Chemical interaction of calcium oxide and calcium hydroxide with CO₂ during mechanical activation. *Inorganic Materials*. 2005. 41(10). Pp. 1073–1079. DOI: 10.1007/s10789-005-0263-1.
25. Erofeev, V.T., Rodin, A.I., Kravchuk, A.S., Kaznacheev, S.V., Zaharova, E.A. Biostable silicic rock-based glass ceramic foams. *Magazine of Civil Engineering*. 2018. 84(8). Pp. 48–56. DOI: 10.18720/MCE.84.5.
26. Yuan, W., Li, J., Zhang, Q., Saito, F. Innovated application of mechanical activation to separate lead from scrap cathode ray tube funnel glass. *Environmental Science and Technology*. 2012. 46(7). Pp. 4109–4114. DOI: 10.1021/es204387a.
27. Yuan, W., Li, J., Zhang, Q., Saito, F., Yang, B. Lead recovery from cathode ray tube funnel glass with mechanical activation. *Journal of the Air and Waste Management Association*. 2013. 63(1). Pp. 2–10. DOI: 10.1080/10962247.2012.711796.
28. Erofeev, V.T., Rodin, A.I., Yakunin, V.V., Tuvin, M.N. Structure, composition and properties of geopolymers from mineral wool waste. *Magazine of Civil Engineering*. 2019. 90(6). Pp. 3–14. DOI: 10.18720/MCE.90.1.
29. Chukin G. D. Himiya poverhnosti i stroenie dispersnogo kremnezema [Surface chemistry and structure of dispersed silica]. Moscow: Printing house Paladin, 2008. 172 p. (rus)

Contacts:

Vladimir Erofeev, a_l_rodin@mail.ru

Alexander Rodin, a_l_rodin@mail.ru

Viktor Bochkin, sovelitnew@mail.ru

Anatolij Ermakov, anatolij.ermakov97@mail.ru